ACS Chemical Neuroscience

Research Article

pubs.acs.org/chemneuro

Development and Validation of a Thallium Flux-Based Functional Assay for the Sodium Channel NaV1.7 and Its Utility for Lead Discovery and Compound Profiling

Yu Du,[†] Emily Days,[‡] Ian Romaine,[§] Kris K. Abney,[†,⊥] Kristian Kaufmann,[†] Gary Sulikowski,[‡,§] Shaun Stauffer,[†,‡,§] Craig W. Lindsley,[†,‡,§,∥] and C. David Weaver*[,†,‡]

[†]Department of Pharmacology, [‡]Institute of Chemical Biology, [§]Department of Chemistry, [∥]Center for Neuroscience Drug Discovery, Vanderbilt University School of Medicine, Nashville, Tennessee 37232, United States

[⊥]Meharry Medical College Program in Pharmacology, Nashville, Tennessee 37208, United States

Supporting Information

ABSTRACT: Ion channels are critical for life, and they are targets of numerous drugs. The sequencing of the human genome has revealed the existence of hundreds of different ion channel subunits capable of forming thousands of ion channels. In the face of this diversity, we only have a few selective small-molecule tools to aid in our understanding of the role specific ion channels in physiology which may in turn help illuminate their therapeutic potential. Although the advent of automated electrophysiology has increased the rate at which we can screen for and characterize ion channel modulators, the technique's high per-measurement cost and moderate throughput compared to other high-throughput screening approaches limit its utility for large-scale high-throughput screening. Therefore, lower cost, more rapid techniques are needed. While ion channel types capable of fluxing calcium are well-served by low cost, very high-throughput fluorescence-based assays, other channel types such as sodium channels remain underserved by present functional assay techniques. In order to address this shortcoming, we have developed a thallium flux-based assay for sodium channels using the NaV1.7 channel as a model target. We show that the assay is able to rapidly and cost-effectively identify NaV1.7 inhibitors thus providing a new method useful for the discovery and profiling of sodium channel modulators.

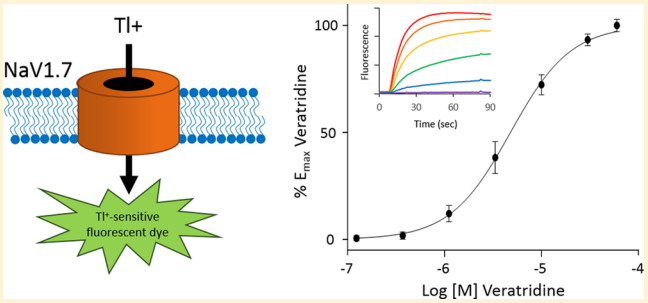

KEYWORDS: *High-throughput screening, sodium channel, thallium flux, drug discovery*

Ion channels are of critical physiological importance. By allowing the facile passage of ions across cellular membranes, they perform functions as diverse as controlling cellular excitability to maintaining solute balance. Most ion channels discriminate between the ions that they conduct with many channels displaying preference for sodium (Na^+), potassium (K^+), calcium (Ca^{2+}), or other ionic species. Ion channels can be regulated by neurotransmitters, membrane lipids, phosphorylation, transmembrane potential, as well as various peptides and small molecules. Through peptide and small molecule modulation, ion channels are utilized as therapeutic targets for a variety of indications including local anesthesia, epilepsy, bipolar disorder, pain management, blood pressure regulation, glucose homeostasis, and others. In fact, drugs targeted toward ion channels make up approximately a tenth of pharmaceuticals[1−3] and ion channels are also major targets of insecticides.[4−6] However, unwanted ion channel modulation can also lead to dose-limiting and sometimes lethal side effects of drugs, thus profiling would-be therapeutics against panels of ion channel targets has become an important part of the drug discovery and development process.

Recently, genomic sequencing has revealed the existence of over four hundred pore-forming ion channel α-subunits as well as numerous accessory subunits.[7−9] The combinatorial nature of ion channel subunit assembly has the potential to lead to a staggering number of functionally and pharmacologically distinct ion channels. This diversity may offer the opportunity to target discrete subpopulations of ion channels, resulting in therapeutics with a superior balance of efficacy and safety. To date, however, there are only a small number of selective pharmacological tools available to study the vast constellation of ion channels. The discovery and development of new tools will be invaluable in increasing our understanding of ion channels in physiology and pathophysiology and may help identify distinct ion channel subunit configurations as targets for new and improved therapies.

The development of patch-clamp electrophysiology has enabled scientists to measure and characterize the activity of

Received: January 5, 2015
Revised: April 14, 2015
Published: April 16, 2015

DOI: 10.1021/acschemneuro.5b00004
ACS Chem. Neurosci. 2015, 6, 871−878

many ion channels. While excelling in resolving power and flexibility, for much of its history the patch clamp technique has been a laborious and exceedingly slow process. The low-throughput of patch-clamp and two-electrode voltage clamp, used to measure the activity of channels expressed in *Xenopus laevis* oocytes, has greatly limited the utility of these techniques to discover novel ion channel modulators. Recently, the advent of multichannel, automated, voltage-clamp instruments has opened the door to screening larger libraries of compounds.[10−12] Unfortunately, automated electrophysiology is still quite expensive and is present in relatively few laboratories. In addition, high-throughput electrophysiology requires that cells are detached from their substrate and held in suspension in order to be loaded into the screening instrument, a process that may introduce unwanted changes in ion channel structure and pharmacology compared to techniques that are amenable to studying channels in cells that are growing on a substrate. Thus, while automated electrophysiology represents a substantial advancement in ion channel screening, significant limitations remain.

Therefore, higher-throughput, less expensive, and more broadly cell-compatible optical techniques are valuable alternatives to automated electrophysiology. For many years, Ca^{2+} channels and nonselective cation channels capable of conducting Ca^{2+} have been well-served by Ca^{+}-sensitive fluorescent dyes (e.g., Fluo-4) paired with kinetic imaging plate readers (e.g., Hamamatsu FDSS, and Molecular Devices FLIPR) for high-throughput screening (HTS).[13−16] More recently, the development of the fluorescence-based thallium (Tl^{+})-flux approach, using dyes like Thallos and FluxOR, has proven valuable for HTS of K^{+} channels[17−27] and electroneutral transporters such as K^{+}-coupled chloride cotransporters (KCC) and Na^{+} and K^{+}-coupled chloride cotransporters (NKCC).[28,29]

Of the ion channels on which much basic research and drug discovery interest is focused, sodium Na^{+} channels have been among the least amenable to HTS. Even though voltage-gated Na^{+} channels are the targets of many drugs and insecticides (e.g, lidocaine and pyrethrins, respectively) the development of Na^{+}-sensitive fluorescent dyes suitable for HTS has largely been unsuccessful. A number of crown-ether-based fluorescent Na^{+}-sensitive dyes (e.g., SBFI and CoroNa dyes) have been synthesized over the years, but these dyes are not well-suited for HTS due to low sensitivity and poor signal-to-background. In the absence of HTS-compatible Na^{+}-sensitive dyes, researchers have been left with (1) radioligand-displacement assays which do not measure receptor function and have the prerequisite of an appropriate radioligand, (2) radioactive ion flux assays which have very poor temporal sensitivity, can only assess activity at a fixed time point, and are difficult to scale for high-throughput screening, and (3) fluorescence-based voltage-sensitive dyes (e.g., DiBAC).[30−32] Although a substantial improvement over binding or radioactive ion flux assays, voltages-sensitive dyes measure the changes in transmembrane potential resulting from ion flux instead of directly measuring ion flux. Because of this fact, voltage-sensitive dyes have many limitations compared to dyes that more directly measure ion flux: (1) Because of the relationship of current to voltage described by Ohm's law, where voltage equals current times resistance ($V = IR$), voltage-sensitive dyes can be very sensitive in situations where cellular membrane resistance is high. Under these conditions only a small proportion of ion channels may need to be active in order to control membrane potential leading to high Hill slopes as previously observed.[30] Conversely, voltage-sensitive dyes can be insensitive to ion channel inhibitors in situations where cellular membrane resistance is low. Under these conditions a large proportion of ion channels may need to be inhibited to result in a change in membrane potential resulting in large right-shifts in apparent potency potentially leading to high false-negative rates. (2) Related to point (1), the target of interest must control the membrane potential in the assay and thus target expression level may have a greater effect on membrane potential-based assays compared to ion flux assays. (3) Because voltage-sensitive dyes can be modulated by not only the target of interest, but any event that changes membrane potential, false positive rates can also be very high. (4) The requirement for extracellular quenching/masking dyes to suppress high background fluorescence associated with voltage-sensitive dyes can introduce unwanted effects when the masking dyes alter cellular physiology or interact directly with the target of interest.

In an attempt to address some of the weaknesses in Na^{+} channel screening approaches, we developed an HTS-compatible fluorescence-based flux assay system using the Tl^{+}-flux approach. We chose the voltage-gated sodium channel NaV1.7 as a model system since it has recently garnered much attention as a potential target of therapeutic intervention for pain.[33] NaV1.7 is associated with two human disease phenotypes. A loss of function results in an insensitivity to visceral pain,[34] while a gain of function results in a chronic pain syndromes.[35] Herein we describe the development, validation, and use of a Tl^{+} flux assay for NaV1.7.

RESULTS AND DISCUSSION

Previous work has demonstrated that Na^{+} channels are Tl^{+} permeant.[36] This observation prompted us to determine whether a Tl^{+} flux assay approach could prove to be an effective technique for measuring the activity of Na^{+} channels in an HTS-compatible format. Using a NaV1.7-expressing HEK-293 cell line loaded with the Tl^{+}-sensitive fluorescent dye, Thallos, we varied concentrations of Tl^{+} and K^{+} in assay buffers searching for conditions that would provide a robust signal. Under all conditions tested, we observed very little increase in Tl^{+} flux compared to untransfected HEK-293 cells. These observations were not surprising because of the rapid inactivation of NaV1.7, our modest data acquisition rate (1 Hz), and our inability to rapidly and uniformly depolarize the cell population in 384-well assay plates. However, when we tested the same conditions using the known inhibitor of NaV inactivation, veratridine,[37] we observed robust Tl^{+} flux in the NaV1.7-expressing cell line but not in untransfected cells (Supporting Information, Figure 1a). The veratridine-evoked Tl^{+} flux was saturable and concentration-dependent with a measured EC_{50} of 4.8 μM and a Hill slope of 1.4 (Figure 1).

Before continuing Tl^{+} flux assay development for NaV1.7, we compared the Tl^{+} flux-based approach to the recently developed Na^{+}-sensitive fluorescent dye, Asante Natrium Green-2 (ANG-2, TEFlabs). With optimized conditions for both dyes, the Tl^{+} flux method produced dramatically larger signal-to-background values (Supporting Information, Figure 2s). Under conditions where Thallos and ANG-2 produced identical background-adjusted initial fluorescence values, ANG-2 was only able to attain an increase in the fluorescence ratio (F/F_0) of 1.1 while Thallos achieved an F/F_0 value of 2.0. Thus, while ANG-2 offers the appeal of Na^{+} selectivity, the very low signal-to-background severely limits its utility in HTS. A potential criticism of the Tl^{+} flux approach is that Tl^{+} can enter

DOI: 10.1021/acschemneuro.5b00004
ACS Chem. Neurosci. 2015, 6, 871−878

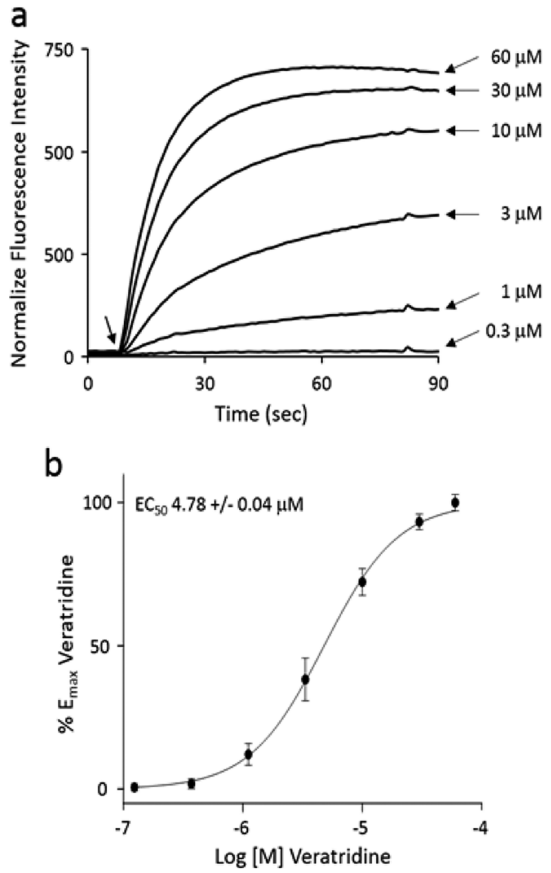

Figure 1. Concentration-dependent efficacy of veratridine in NaV1.7-expressing HEK-293 cells. Shown in (a) are a representative set of traces from a Tl^+ flux assay in NaV1.7-expressing HEK-293 cells in the presence of varying concentrations of veratridine. The arrow shows the point of addition of veratridine in Tl^+-containing stimulus buffer. Shown in (b) are averaged data from three independent experiments fit using a four-parameter logistic equation. The *Y*-axis represents the change in the slope of traces in (a) relative to the slope observed with a maximally effective concentration of veratridine. The calculated potency is 4.78 ± 0.04 μM with a Hill slope of 1.39± 0.14.

the cell through a variety of pathways native to HEK cells (e.g., the Na^+/K^+ ATPase). However, NaV1.7-expressing HEK cells showed 5-fold higher Tl^+ flux compared to untransfected HEK-293 cells. Thus, in our NaV1.7 assay, the native Tl^+ flux is no more of a limitation than when Tl^+ flux assays have been used successfully to perform HTS on cells overexpressing K^+ channels[17,18,20,23,26] or K^+-conducting transporters.[28] Based on our observations that we could observe robust Tl^+ flux in NaV1.7-expressing cells and that the signal was superior to the state-of-the art Na^+-sensitive dye, we proceeded to optimize Tl^+ flux conditions for the detection of NaV1.7 inhibitors.

To investigate the ability of the Tl^+ flux technique to detect NaV1.7 inhibitors, we first determined that a final Tl^+ concentration of 3.8 mM in the presence of 25 mM potassium and 10 μM veratridine produced Tl^+ flux that was approximately 80% of the maximum observed response obtained with 60 μM veratridine under the same concentrations of Tl^+ and K^+. We chose an EC_{80} concentration of veratridine to allow detection of a broader range of types of NaV1.7 modulators, including those that either compete with or alter the channel's affinity for veratridine or those that can activate the channel. This approach seemed prudent based on the experience of Felix and colleagues who noted that the NaV1.7 inhibitor, Co102862, likely competes with veratridine.[30] In our initial studies we demonstrated that the NaV1.7 inhibitor, TC-N 1752,[37] shows a concentration-dependent ability to inhibit Tl^+ flux in NaV1.7-expressing cells in the presence of an EC_{80} concentration of veratridine (Figure 2).

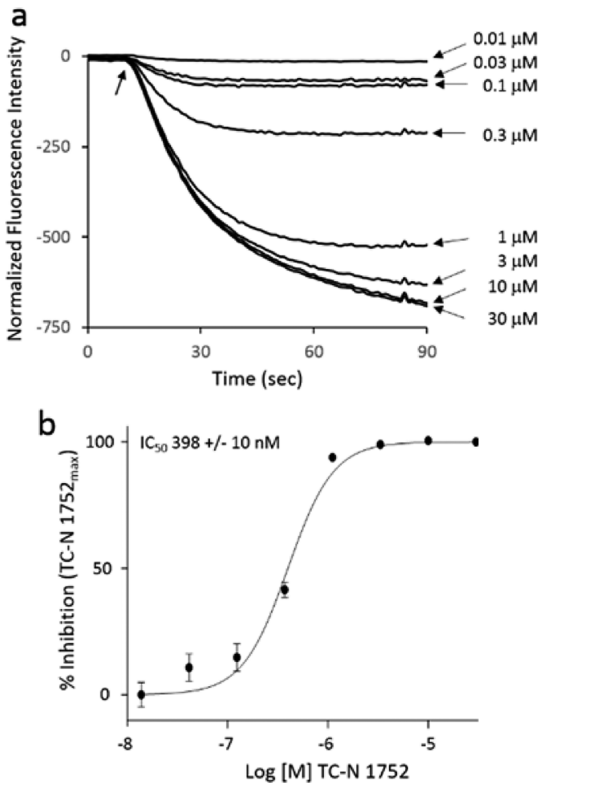

Figure 2. Concentration-dependent efficacy of TC-N 1752 in veratridine-treated, NaV1.7-expressing HEK-293 cells. Shown in (a) are a representative set of traces from a Tl^+ flux assay in NaV1.7-expressing HEK-293 cells treated with an EC_{80} concentration of veratridine in the presence of varying concentrations of TC-N 1752. The traces shown result from the subtraction of the vehicle control (no inhibitor) values from the values at each of the various inhibitor concentrations revealing inhibitor-mediated decrease in Tl^+ flux relative to the no inhibitor condition. The arrow shows the point of addition of veratridine in Tl^+-containing stimulus buffer. Shown in (b) are averaged data from three independent experiments fit using a four-parameter logistic equation. The calculated potency is 398 ± 10 nM with a Hill slope of 1.91 ± 0.16.

The 398 nM measured potency of TC-N 1752 under our assay conditions is similar to values reported using whole-cell voltage clamp electrophysiology (170 nM).[38] Encouraged by these results, we tested six other compounds known to inhibit the activity of NaV1.7: carbamazepine, lidocaine, bupivacaine, ranolazine, mibefradil, and tetrodotoxin. Using the Tl^+ flux technique, most compounds demonstrated a shift in potency that averaged 4-fold compared to published voltage-clamp measurements.[39−45] However, potencies obtained from both techniques correlate very strongly (R^2 = 0.98), and the rank order of potencies measured using Tl^+ flux and whole-cell voltage clamp matched across this structurally diverse set of NaV1.7 inhibitors. Due to the sensitivity of some NaV inhibitors to the state of the channel (e.g., open versus closed, "resting" versus inactivated) care must be taken not to overinterpret the data presented in Figure 3, particularly since

DOI: 10.1021/acschemneuro.5b00004
ACS Chem. Neurosci. 2015, 6, 871−878

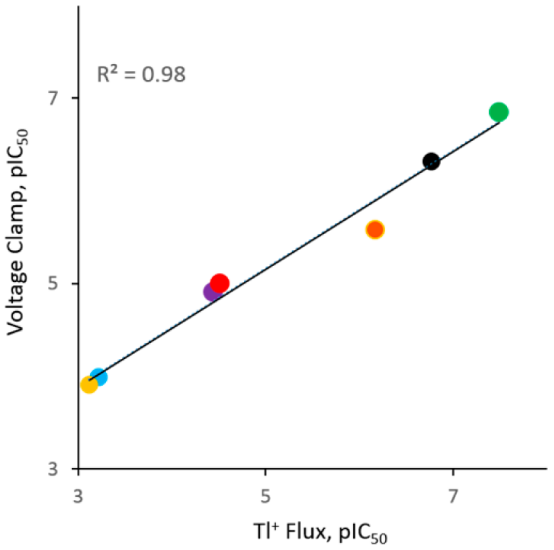

Figure 3. Comparison of potency values obtained using the Tl^+ flux technique with those obtained using voltage-clamp. The values shown for the Tl^+ flux assay were obtained from three independent experiments. The values shown for the voltage-clamp electrophysiology assays were obtained from the literature. The compounds tested were, from left to right: carbamazepine (yellow), lidocaine (blue), bupivacaine (purple), ranolaxine (red), mibefradil (orange), TC-N 1752 (black), and tetrodotoxin (green).

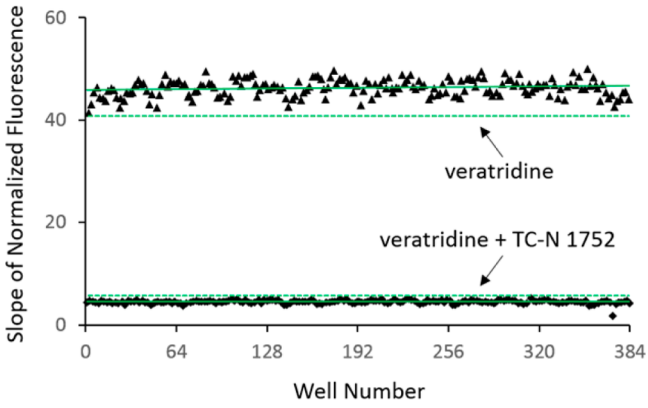

Figure 4. Well-to-well uniformity of TC-N 1752-mediated inhibition of veratridine-evoked Tl^+ flux in NaV1.7-expressing HEK-293 cells. Shown is a representative scatter plot of slope values obtained from 10 μM veratridine-treated or 10 μM veratridine and 10 μM TC-N 1752-treated wells. The mean slope of each sample population is indicated with solid lines, and three standard deviations from the population mean is indicated with dashed lines.

the experimenter's ability to control the channel's state is much more limited using the Tl^+ flux approach compared to voltage-clamp electrophysiology. The main value of the data presented in Figure 3 is to demonstrate the Tl^+ flux technique is capable of detecting the NaV1.7 inhibitory activity of compounds from a variety of structural classes spanning a broad range of potencies.

Following these studies, we set out to determine the suitability of this assay for HTS by exploring its well-to-well and day-to-day variability in 384-well plates under our optimized assay conditions. Supporting Information Figure 3s shows a representative result of testing a 384-well plate where every other well was exposed to either assay buffer or assay buffer containing 10 μM veratridine using our optimized assay conditions. *z*-Factor calculations[46] produced an average *z*-factor of 0.70 ± 0.07 in experiments conducted over three separate days. In a similar experiment, we tested every other well in the presence of either 10 μM veratridine or 10 μM veratridine plus 10 μM TC-N 1752, where the TC-N 1752 was added in advance of the veratridine-containing Tl^+ stimulus buffer (Figure 4). Under these conditions, *z*-factor calculations produced an average *z*-factor of 0.69 ± 0.03 in experiments conducted over three separate days. A *z*-factor of 0.5 is typically considered indicative that an assay is suitable for large scale HTS screens where each compound is tested only once.

Since our *z*-factors were uniformly above 0.5 for all plates tested, we performed a pilot screen on the MicroSource Spectrum collection, which is a collection of approximately 2300 compounds enriched for those with known activities at a variety of targets including ion channels. Since some sodium channel inhibitors (e.g., bupivacaine) also inhibit the G-protein-activated inward-rectifying potassium channel (GIRK, K_{ir3}),[47] we also profiled a set of approximately 400 compounds that were on hand from our efforts to develop small molecule modulators of GIRK channels[17,48−50]. We tested all of these compounds at a 10 μM concentration under the assay conditions we established for detecting NaV1.7 inhibitors described above. We selected 164 hits that showed a decrease in veratridine-evoked Tl^+ flux with a z-score of 3 or greater. When these compounds were retested against NaV1.7-expressing HEK-293 cells and untransfected HEK-293 cells, 145 (88%) of the compounds displayed activity unique to the NaV1.7-expressiing cells. Although the 5.4 % hit rate observe for the pilot screen may seem high, it is not surprising considering that both the Spectrum collection and the GIRK modulator library are highly enriched for ion channel modulators. In particular, the GIRK-targeted collection showed a verified hit rate of >25% of the compounds in the library. The hit list contained many expected ion channel inhibitor scaffolds including the "caine" family local anesthetics (e.g., butacaine), tricyclic antidepressants and dihypropyridines. Of the verified hits from both libraries, we selected a set of 32 compounds for further analysis. These compounds were selected based on a combination of their activity in the Tl^+ flux assay as well as structural similarity to either compounds known to inhibit Na^+ channels (e.g., members of the "caine" family) or those without prior reported Na^+ channel inhibitory properties (e.g., phenolphthalein and the compounds from the GIRK channel modulator library such as VU0464120). These 32 compounds were obtained in powdered form and tested for their ability to produce concentration-dependent inhibition of veratridine-evoked Tl^+ flux in NaV1.7-expressing cells. We found that 27 of the compounds tested (84%) produced concentration-dependent efficacy with apparent potencies ranging from 1 to 20 μM. From the group of 27 compounds, we selected 4 compounds, each from a different structural class, for testing using whole-cell voltage-clamp electrophysiology. Of the compounds chosen, VU0464120, phenolphthalein, and MCFD00168650 showed potencies obtained using the Tl+ flux assay of ∼1−2 μM, while CID 6044366 had a potency of >20 μM. As shown in Figure 5, the inhibition profile of the compounds tested at a concentration of 30 μM closely matches for the two techniques with the more potent compounds showing near complete inhibition in both assays systems while the low-potency compound, CID6044366, showed only modest inhibition in both assays.

DOI: 10.1021/acschemneuro.5b00004
ACS Chem. Neurosci. 2015, 6, 871−878

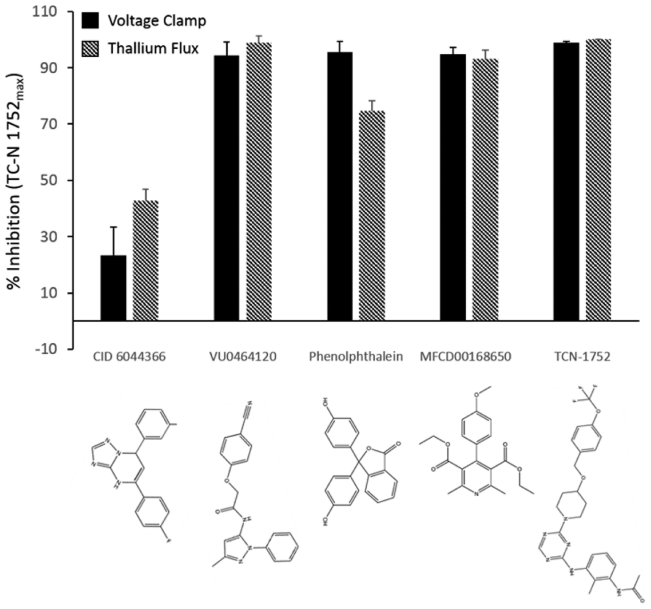

Figure 5. Comparison of efficacy of selected compounds using Tl^+ flux and whole-cell voltage-clamp assays. Shown are a selection of compounds observed to have varying degrees of inhibition of NaV1.7 measured using the Tl^+ flux assay. The bars show the average inhibition (± SEM) observed using whole-cell voltage clamp (black bars) and Tl^+ flux (hatched bars). Percent inhibition was normalized to the degree of inhibition observed with a maximally effective concentration of TCN-1752, 30 μM.

In summary, we have demonstrated that a fluorescence-based Tl^+ flux approach can be used to detect inhibitors of the NaV1.7 sodium channel when the channel's inactivation has been inhibited by veratridine. The Tl^+ flux assay shows excellent well-to-well and plate-to-plate performance with z-factors well above 0.5. When used for compound screening in 384-well plates, we found that the Tl^+ flux assay was able to detect NaV1.7 inhibitors spanning a range of structural classes and that detection of low potency compounds, such as CID6044366, was possible. The Tl^+ flux assay showed a less steep Hill slope for veratridine compared to a voltage-sensitive dye approach,[30] consistent with the prediction that voltage-sensitive dye measurements would be more sensitive to changes in the activity of a small number of channels when membrane resistance is high. However, when comparing the three reference compounds that were common between the present work and the work of Felix and colleagues[30] (carbamazepine, lidocaine, tetrodotoxin), the two approaches showed the same rank order of potency. Thus, based on this limited set of data, both assays appear capable of detecting NaV1.7 inhibitors from a variety of structural classes and potencies. However, the advantages remain that the Tl^+ flux assay will be less sensitive to the target channel expression level, does not require the target of interest to control the membrane potential in the assay, and does not require the presence of potentially interfering extracellular quencher/masking dyes. Compared to other medium and high-throughput approaches for detecting sodium channel modulators, the Tl^+ flux approach is very cost-effective: ~7 cents/well in 384-well format compared to ~87 cents/well for a typical automated electrophysiology platform, ~24 cents/well for the Invitrogen VSP system, and ~25 cents/well for the Molecular Devices FLIPR Membrane Potential Assay Kit. All of these features may prove particularly advantageous when developing assays for use in large-scale high-throughput screening.

Based on our present findings, we predict that the assay can further be utilized in both ligand discovery and selectivity profiling for a variety of voltage-gated and non-voltage-gated sodium channels, such as NaV1.1-NaV1.9 and ENaC, respectively. In order to explore broader utility of the Tl^+ flux assay for supporting hits-to-leads, lead-optimization, and compound selectivity testing, future studies will address the ability of the Tl^+ flux assay to accurately rank the potencies of compounds within a structurally related series of compounds in order to determine whether the technique can serve as a surrogate for voltage-clamp in support of rapid and cost-effective development of structure–activity relationships in coordination with medicinal chemistry efforts. In a related vein, future studies will also address whether the assay is capable of resolving differences in a compound's activity at a target of interest versus prospective "anti-targets". For instance, in a scenario where an NaV1.7 inhibitor is desired, a Tl^+ flux-based profiling assay would be useful for rapidly testing "hits" at NaV1.5, NaV1.6, and so forth as a means of post-HTS compound prioritization and would be of further utility to monitor compound selectivity as part of hits-to-leads or lead-development studies. Although the ability to use the Tl^+ flux assay to support development of structure–activity relationships and to allow high-resolution selectivity profiling would greatly extend the utility of the technique, the ability of the Tl^+ flux assay to rapidly and cost-effectively provide a means for high-throughput discovery of Na^+ channel modulators will undoubtedly prove valuable.

METHODS

Cell Lines and Culture Condition. SCN9A (NaV1.7) cloned into pCMV6-puro was purchased from OriGene (Rockville, MD). A NaV1.7 expressing cell line, N7A, was generated by transfecting the SCN9A-containing plasmid into HEK-293 cells (ATCC# CRL-1573, Manassas, VA) using FuGENE 6 (Promega, Madison, WI). Following antibiotic selection in puromycin-containing medium, (3 μg/mL) the antibiotic resistant cells were subjected to limiting dilution with 0.8 cells/well were place into ~700 wells in 384-well plates. Wells where cell colonies formed were harvested using TrypLE Express (Life Technologies, Carlsbad, CA), replica plated into 384-well plates, and assayed as described below. Clones demonstrating a high-degree of veratridine-sensitive Tl^+ flux were selected for further investigation, and one of the most highly expressing clones, N7A, was used for experiments in this study. For validation of expression of NaV1.7, clonal cell line N7A cells at ~80% confluence were harvested from a T175 flask using TrypLE Expressed and sedimented by centrifugation at 500*g* for 2 min at room temperature. The supernatant solution was removed and the pellet was extracted with 500 μL of RIPA buffer (Sigma-Aldrich, St. Louis, MO). Then 15 μg protein/well of sample was separated by SDS-PAGE and blotted to a PVDF membrane. The blot was blocked with 5% (w/v) nonfat dry milk in 150 mM NaCl, 50 mM Tris-HCl, pH7.5 (TBS)-containing 0.05% Tween 20 for 1 h at room temperature and then probed with a 1:500 dilution of an anti-NaV1.7 antibody (TA329033, Origene, Rockville, MD) in TBS-containing 0.05% Tween 20 for 6 h at 4 °C. Following primary antibody incubation, the blot was washed with TBS-containing 0.05% Tween 20 after which a 1:10 000 dilution of horseradish peroxidase-conjugated goat anti-rabbit IgG (Jackson immuno-Research Laboratories, West Grove, PA) was added and incubated for 1 h at room temperature. Following incubation, the blot was washed in TBS-containing 0.05% Tween 20. Secondary antibody signal was detected using SuperSignal West Pico Chemiluminescent substrate (Life Technologies, Carlsbad, CA).

DOI: 10.1021/acschemneuro.5b00004
ACS Chem. Neurosci. 2015, 6, 871–878

Cells were cultured at 37 °C and 5% CO_2. Cell culture medium consisted of Minimal Essential Medium (Mediatech, Manassas, VA) containing 1× Glutagro (Mediatech, Manassas, VA) and 10% (v/v) heat-inactivated fetal bovine serum (Life Technologies, Carlsbad, CA).

Thallium Flux Assays. For Tl^+ flux assays of NaV1.7-expressing cells, cells were dislodged from tissue culture flasks using TrypLE Express, transferred to a 50 mL centrifuge tube, and centrifuged at 500*g* for 2 min. The supernatant solution was removed by aspiration, and the pellet was resuspended at a concentration of ~1000 cells/μL in cell culture medium. Then 20 μL/well of the cell suspension was transferred to 384-well, amine-coated assay plates (cat# 354719, BD, Franklin Lakes, NJ) using an electronic multichannel pipet. Plated cells were incubated overnight in a humidified 5% CO_2 cell culture incubator at 37 °C. After overnight incubation, the cell culture medium was replaced with 20 μL/well of dye-loading solution consisting of assay buffer (Hanks Balanced Salt Solution (Mediatech, Manassas, VA) plus 20 mM HEPES, pH 7.3), 0.04% (w/v) Pluronic F-127 (Sigma-Aldrich, St. Louis, MO), and 1 μM of the thallium-sensitive dye Thallos-AM (TEFlabs, Austin, TX). Following a 45 min incubation at room temperature, the dye-loading solution was replaced with 20 μL/well of assay buffer, and the plates were loaded into a Hamamatsu FDSS 6000 (Bridgewater, NJ). Data were acquired at 1 Hz (excitation 470 ± 20 nm, emission 540 ± 30 nm) for 10 s, followed by the addition of 20 μL/well of test compounds (prepared as described below), followed by an additional 10 min of data collection. At the 10 min mark, 10 μL/well of a Tl^+ stimulus buffer was added and data collection continued for an additional 5 min. The Tl^+ stimulus buffer consisted of 125 mM $KHCO_3$, 1.8 mM $CaSO_4$, 1 mM $MgSO_4$, 5 mM glucose, 9.5 mM Tl_2SO_4, 10 mM HEPES, pH 7.4, and varying concentrations of veratridine (Sigma-Aldrich, St. Louis, MO) at 5-fold above the intended final concentration.

Compounds for pilot screening were from the Spectrum Collection (MicroSource, Gaylordsville, CT). Compounds for further characterization were purchased through Aldrich Market Select (www.AldrichMarketSelect.com) or ChemBridge (San Diego, CA). TC-N 1752 was purchased from Tocris (Minneapolis, MN). Stock solutions of compounds (10 or 30 mM) were prepared by dissolving the compounds in dimethyl sulfoxide (DMSO, Sigma-Aldrich, St. Louis, MO). For Tl^+-flux assays, stock compound solutions in 384-well plates were serially diluted in DMSO using a Bravo liquid handler (Agilent, Technologies, Santa Clara, CA) and then transferred to another 384-well plate using an Echo 555 plate reformatter (Labcyte, Sunnyvale, CA). The compounds were then diluted to 2-fold above their final concentration in assay buffer. For electrophysiology assays, stock solutions were serially diluted by hand in DMSO and then further diluted in electrophysiology external solutions (described below).

Fluorescence data were normalized by dividing the fluorescence values at each time point in each well by the average of that well's first five time points (F/F_0). In all instances, with the exception of Supporting Information Figure 2s, the F/F_0 value was multiplied by average initial fluorescent values for all wells on the assay plate to arrive at "normalized fluorescence intensity". In all instances, with the exception of Figure 1s, the normalized values at each time point from the vehicle-control condition (no veratridine or no inhibitor, as appropriate) was subtracted from the values obtained under the test compound conditions to reveal time-dependent, test condition-mediated changes in Tl^+ flux. Tl^+ flux data were quantified by measuring the slope of the increase in fluorescence over a 10 s period beginning 2 s after the addition of Tl^+ stimulus buffer. Correlation plots and fits to concentration series experiments were performed in Excel (Microsoft, Redmond, WA) using XLfit (IDBS, London, UK). All data represent the average of at least three independent experiments per assay condition.

The Na^+ flux assay of NaV1.7-expressing cells was performed in a similar fashion to the Tl^+ flux assay described above; Thallos was replaced with 4 μM Asante Natrium Green-AM (ANG-2 AM, TEFlabs, Austin, TX). The stimulus buffer in this assay was composed of assay buffer and veratridine at 5-fold above the desired final concentration. Data collection was performed using the Hamamatsu FDSS 6000 as described above.

Electrophysiology. Whole-cell voltage-clamp experiments were conducted using a Port-a-Patch (Nanion, Munich, Germany) connected to a HEKA EPC-10 amplifier (Lambrecht/Pfalz, Germany) under the control of PatchMaster software. NaV1.7-expressing cells at ~85% confluent cells were dislodged from a T75 flask using TrypLE Express and resuspended in 2 mL of extracellular solution (140 mM NaCl, 4 mM KCl, 1 mM MgCl2, 2 mM CaCl2, 5 mM D-glucose, 10 mM HEPES, pH7.4, 298 mOsmol). The internal solution contained 50 mM CsCl, 10 mM NaCl, 60 mM CsF, 20 mM EGTA, 10 mM HEPES/CsOH, pH 7.2, 285 mOsmol). Cells were captured, seals were formed, and whole-cell access was established under the control of the PatchMaster software according to the manufacturer's instructions. For recording currents, cells were held at −100 mV and depolarized with a series of 10 ms pulses from −100 to 5 mV in 5 mV steps at a frequency of 5 Hz. Data were acquired at 10 kHz and filtered at 2.9 kHz. Average series resistance R_s was 5.5 ± 1.8 MΩ. Series resistance was partially compensated for using the EPC-10s series resistance compensation circuit resulting in an average voltage error of 3.1 ± 1.6 mV. Pipette and cellular capacitance were compensated for using the EPC-10s Auto C-fast and Auto C-slow, respectively. For each cell, current amplitudes were obtained in extracellular solution without test compounds followed by addition of test compounds dissolved in extracellular solution at concentrations of 30 μM. The pulse protocol was repeated until no further changes in current amplitude were noted. After each compound had reached its maximum inhibitory effect, test compounds were replaced with 30 μM TC-N 1752 and the pulse protocol was repeated until stable current amplitudes were obtained.

Electrophysiology data were analyzed by measuring current amplitudes at −20 mV after compound effects had reached steady-state levels. Current amplitudes were normalized based on measurements of cellular capacitance and expressed as current densities, pA/pF. On a per-cell basis, these current densities were further normalized to the effect of TC-N 1752 on the same cells and expressed as percent of inhibition. The degree of current inhibition observed with 30 μM TC-N 1752 was defined as 100% inhibition. All data represent the average of at least three independent experiments per assay condition.

■ ASSOCIATED CONTENT

Supporting Information

(1) Tl^+ flux in the presence of 10 μM veratridine in NaV1.7-expressing and untransfected HEK-293 cells. (2) Western blot of protein extracts from NaV1.7-expressing and untransfected HEK-293 cells probed with anti-NaV1.7 antibody. (3) Comparison of veratridine-evoked Na^+ influx detected with Asante Natrium Green and veratridine-evoked Tl^+ influx detected with Thallos in NaV1.7-expressing HEK-93 cells. (4) Well-to-well uniformity of Tl^+ flux in NaV1.7-expressing HEK-293 cells in the presence and absence of 10 μM veratridine. The Supporting Information is available free of charge on the ACS Publications website at DOI: 10.1021/acschemneuro.5b00004.

■ AUTHOR INFORMATION

Corresponding Author

*Mailing address: 459 Preston Research Building, Department of Pharmacology, Vanderbilt University School of Medicine, Nashville, TN 37232.

Author Contributions

Y.D. designed and perform the Tl^+ flux and electrophysiology assays. C.D.W. conceived of the study, provided oversight and management, developed the NaV1.7-expressing cell line, and wrote the manuscript. K.K.A. performed the immunochemistry studies on the NaV1.7-expressing cell line. K.K. developed the WaveGuide data analysis tool used for Tl^+ flux and Na^+ flux data reduction and analysis and assisted in data analysis for the pilot screen. E.D. provided support for cell NaV 1.7 cell line

DOI: 10.1021/acschemneuro.5b00004
ACS Chem. Neurosci. 2015, 6, 871−878

creation, assay validation, and pilot screening. S.S. analyzed hit compound structures and selected compound on which to conduct more in-depth analysis. C.L., G.S., and I.R. designed and synthesized compounds from the GIRK modulator library tested in the pilot screen.

Funding

The Vanderbilt University Department of Pharmacology, the Vanderbilt University Institute of Chemical Biology, and the Vanderbilt Clinical and Translational Science Award VICTR program.

Notes

The authors declare the following competing financial interest(s): C. David Weaver receives royalties from TEFlabs through the sale of Thallos which is licensed to TEFlabs by Vanderbilt University.

■ ACKNOWLEDGMENTS

The authors thank Krystian Kozek for helpful comments during the preparation of the manuscript. The authors also appreciate support from the Vanderbilt University Department of Pharmacology, the Vanderbilt University Institute of Chemical Biology, the Vanderbilt Clinical and Translational Science Award (CTSA) award No. UL1TR000445 from the National Center for Advancing Translational Sciences, the Vanderbilt High-throughput Screening Facility, the Vanderbilt MLPCN Specialized Chemistry Center, and the Vanderbilt Chemical Synthesis Core Facility.

■ REFERENCES

(1) Clare, J.-J. (2010) Targeting Ion Channels for Drug Discovery. *Discovery Med. 9*, 253−260.

(2) Wickenden, A., Priest, B., and Erdemli, G. (2012) Ion channel drug discovery: challenges and future directions. *Future Med. Chem. 4*, 661−679.

(3) Terstappen, G.-C., Roncarati, R., Dunlop, J., and Peri, R. (2010) Screening technologies for ion channel drug discovery. *Future Med. Chem. 2*, 715−730.

(4) Clark, J.-M., and Symington, S.-B. (2011) Advances in the Mode of Action of Pyrethroids. *Top. Curr. Chem. 314*, 49−72.

(5) Casida, J.-E. (2011) Curious about pesticide action. *J. Agric. Food Chem. 59*, 2762−2769.

(6) Casida, J.-E., and Durkin, K.-A. (2013) Neuroactive insecticides: targets, selectivity, resistance, and secondary effects. *Annu. Rev. Entomol. 2013*, 99−117.

(7) Bagal, S.-K., Brown, A.-D., Cox, P.-J., Omoto, K., Owen, R.-M., Pryde, D.-C., Sidders, B., Skerratt, S.-E., Stevens, E.-B., Storer, I.-R., and Swain, N.-A. (2013) Ion Channels as Therapeutic Targets: A Drug Discovery Perspective. *J. Med. Chem. 56*, 593−624.

(8) Jegla, T.-J., Zmasek, C.-M., Batalov, S., and Nayak, S.-K. (2009) Evolution of the human ion channel set. *Comb. Chem. High Throughput Screen 12*, 2−23.

(9) Klassen, T., Davis, C., Goldman, A., Burgess, D., Chen, T., Wheeler, D., McPherson, J., Bourquin, T., Lewis, L., Villasana, D., Morgan, M., Muzny, D., Gibbs, R., and Noebels, J. (2011) Exome sequencing of ion channel genes reveals complex profiles confounding personal risk assessment in epilepsy. *Cell 145*, 1036−1048.

(10) Dunlop, J., Bowlby, M., Peri, R., Vasilyev, D., and Arias, R. (2008) High-throughput electrophysiology: an emerging paradigm for ion-channel screening and physiology. *Nat. Rev. Drug Discovery 7*, 358−368.

(11) Farre, C., Stoelzle, S., Haarmann, C., George, M., Brüggemann, A., and Fertig, N. (2007) Automated ion channel screening: patch clamping made easy. *Expert Opin. Ther. Targets 11*, 557−565.

(12) Castle, N., Printzenhoff, D., Zellmer, S., Antonio, B., Wickenden, A., and Silvia, C. (2009) Sodium channel inhibitor drug discovery using automated high throughput electrophysiology platforms. *Comb. Chem. High Throughput Screening 12*, 107−122.

(13) Lubin, M.-L., Reitz, T.-L., Todd, M.-J., Flores, C.-M., Qin, N., and Xin, H. (2006) A nonadherent cell-based HTS assay for N-type calcium channel using calcium 3 dye. *Assay Drug Dev. Technol. 4*, 689−694.

(14) Kim, Y., Kang, S., Lee, J.-Y., and Rhim, H. (2009) High throughput screening assay of alpha(1G) T-type Ca2+ channels and comparison with patch-clamp studies. Comb. Chem. *High Throughput Screening 12*, 296−302.

(15) Xie, X., Van Deusen, A.-L., Vitko, I., Babu, D.-A., Davies, L.-A., Huynh, N., Cheng, H., Yang, N., Barrett, P.-Q., and Perez-Reyes, E. (2007) Validation of high throughput screening assays against three subtypes of Ca(v)3 T-type channels using molecular and pharmacologic approaches. *Assay Drug Dev. Technol. 5*, 191−203.

(16) Bettini, E., Sava, A., Griffante, C., Carignani, C., Buson, A., Capelli, A.-M., Negri, M., Andreetta, F., Senar-Sancho, S.-A., Guiral, L., and Cardullo, F. (2010) Identification and characterization of novel NMDA receptor antagonists selective for NR2A- over NR2B-containing receptors. *J. Pharmacol. Exp. Ther. 335*, 636−644.

(17) Kaufmann, K., Romaine, I., Days, E., Pascual, C., Malik, A., Yang, L., Zou, B., Du, Y., Sliwoski, G., Morrison, R.-D., Denton, J., Niswender, C.-M., Daniels, J.-S., Sulikowski, G.-A., Xie, X.-S., Lindsley, C. W., and Weaver, C.-D. (2013) ML297 (VU0456810), the first potent and selective activator of the GIRK potassium channel, displays antiepileptic properties in mice. *ACS Chem. Neurosci. 4*, 1278−1286.

(18) Raphemot, R., Lonergan, D.-F., Nguyen, T.-T., Utley, T., Lewis, L. M., Kadakia, R., Weaver, C.-D., Gogliotti, R., Hopkins, C., Lindsley, C.-W., and Denton, J.-S. (2011) Discovery, characterization, and structure-activity relationships of an inhibitor of inward rectifier potassium (Kir) channels with preference for Kir2.3, Kir3.x, and Kir7.1. *Front. Pharmacol. 2*, 75.

(19) Wydeven, N., Fernandez de Velasco, E.-M., Du, Y., Benneyworth, M.-A., Hearing, M.-C., Fischer, R.-A., Thomas, M.-J., Weaver, C.-D., and Wickman, K. (2014) Mechanisms underlying the activation of G-protein-gated inwardly rectifying K+ (GIRK) channels by the novel anxiolytic drug, ML297. *Proc. Natl. Acad. Sci. U. S. A. 111*, 10755−10760.

(20) Yu, H., Wu, M., Townsend, S.-D., Zou, B., Long, S., Daniels, J.-S., McManus, O.-B., Li, M., Lindsley, C.-W., and Hopkins, C.-R. (2011) Discovery, Synthesis, and Structure Activity Relationship of a Series of N-Aryl- bicyclo[2.2.1]heptane-2-carboxamides: Characterization of ML213 as a Novel KCNQ2 and KCNQ4 Potassium Channel Opener. *ACS Chem. Neurosci. 2*, 572−577.

(21) Weaver, C.-D., Harden, D., Dworetzky, S.-I., Robertson, B., and Knox, R.-J. (2004) A Thallium-sensitive, Fluorescence-based Assay for Detecting and Characterizing Potassium Channel Modulators in Mammalian Cells. *J. Biomol. Screen. 9*, 671−677.

(22) Niswender, C.-M., Myers, K.-A., Lou, Q., Ayala, J., Kim, C., Conn, P.-J., and Weaver, C.-D. (2008) Development of a Novel and Direct Assay for High-Throughput Screening of Gi/o-linked GPCRs using Thallium Flux Through GIRK Channels. *J. Mol. Pharm. 73*, 1213−1224.

(23) Lewis, M., Bhave, G., Chauder, B.-A., Banerjee, S., Lornsen, K., Redha, R., Fallen, K., Lindsley, C.-W., Weaver, C.-D., and Denton, J.-S. (2009) High-throughput screening reveals a small-molecule inhibitor of ROMK and Kir7.1. *Mol. Pharmacol. 76*, 1094−103.

(24) Bhave, G., Chauder, B. A., Liu, W., Dawson, E. S., Kadakia, R., Nguyen, T.-T., Lewis, L.-M., Meiler, J., Weaver, C.-D., Satlin, L.-M., Lindsley, C.-W., and Denton, J.-S. (2010) Development of a selective small-molecule inhibitor of Kir1.1, the Renal Outer Medullary Potassium Channel. *Mol. Pharmacol. 79*, 42−50.

(25) Potet, F., Lorinc, A.-N., Chaigne, S., Hopkins, C.-R., Venkataraman, R., Stepanovic, S.-Z., Lewis, L.-M., Days, E., Sidorov, V.-Y., Engers, D.-W., Zou, B., Afshartous, D., George, A.-L., Jr., Campbell, C.-M., Balser, J.-R., Li, M., Baudenbacher, F.-J., Lindsley, C.-W., Weaver, C.-D., and Kupershmidt, S. (2012) Identification and characterization of a compound that protects cardiac tissue from

DOI: 10.1021/acschemneuro.5b00004
ACS Chem. Neurosci. 2015, 6, 871−878

human ether-a-go-go-related gene (hERG)-related, drug-induced Arrhythmias. *J. Biol. Chem. 287*, 39613−39625.
(26) Li, Q., Rottländer, M., Xu, M., Christoffersen, C.-T., Frederiksen, K., Wang, M.-W., and Jensen, H.-S. (2011) Identification of novel KCNQ4 openers by a high-throughput fluorescence-based thallium flux assay. *Anal. Biochem. 418*, 66−72.
(27) Schmalhofer, W.-A., Swensen, A.-M., Thomas, B.-S., Felix, J.-P., Haedo, R.-J., Solly, K., Kiss, L., Kaczorowski, G.-J., and Garcia, M.-L. (2010) A pharmacologically validated, high-capacity, functional thallium flux assay for the human Ether-à-go-go related gene potassium channel. *Assay Drug Dev. Technol. 8*, 714−726.
(28) Delpire, E.-J., Days, E., Lewis, M., Mi, D., Lindsley, C., and Weaver, C.-D. (2009) Small Molecule Screen Identifies Novel Inhibitors of the Neuronal K-Cl cotransporter KCC2. *Proc. Natl. Acad. Sci. U. S. A. 106*, 5383−5388.
(29) Carmosino, M., Rizzo, F., Torretta, S., Procino, G., and Svelto, M. (2013) High-throughput fluorescent-based NKCC functional assay in adherent epithelial cells. *BMC Cell Biol. 14*, 16.
(30) Felix, J.-P., Williams, B.-S., Priest, B.-T., Brochu, R.-M., Dick, I.-E., Warren, V.-A., Yan, L., Slaughter, R.-S., Kaczorowski, G.-J., Smith, M.-M., and Garcia, M.L. (2004) Functional assay of voltage-gated sodium channels using membrane potential-sensitive dyes. *Assay Drug Dev. Technol. 2*, 260−268.
(31) Vickery, R.-G., Amagasu, S.-M., Chang, R., Mai, N., Kaufman, E., Martin, J., Hembrador, J., O'Keefe, M.-D., Gee, C., Marquess, D., and Smith, J.-A. (2004) Comparison of the pharmacological properties of rat Na(V)1.8 with rat Na(V)1.2a and human Na(V)1.5 voltage-gated sodium channel subtypes using a membrane potential sensitive dye and FLIPR(R). *Recept. Channels 10*, 11−23.
(32) Chen, M.-X., Gatfield, K., Ward, E., Downie, D., Sneddon, H.-F., Walsh, S., Powell, A.-J., Laine, D., Carr, M., and Trezise, D. (2015) Validation and Optimization of Novel High-Throughput Assays for Human Epithelial Sodium Channels. *J. Biomol. Screening 20*, 242−253 DOI: 10.1177/1087057114552399.
(33) Clare, J.-J. (2010) Targeting voltage-gated sodium channels for pain therapy. *Expert Opin. Invest. Drugs 19*, 45−62.
(34) Goldberg, Y.-P., MacFarlane, J., MacDonald, M.-L., Thompson, J., Dube, M.-P., Mattice, M., Fraser, R., Young, C., Hossain, S., Pape, T., Payne, B., Radomski, C., Donaldson, G., Ives, E., Cox, J., Younghusband, H.-B., Green, R., Duff, A., Boltshauser, E., Grinspan, G.-A., Dimon, J.-H., Sibley, B.-G., Andria, G., Toscano, E., Kerdraon, J., Bowsher, D., Pimstone, S.-N., Samuels, M.-E., Sherrington, R., and Hayden, M.-R. (2007) Loss-of-function mutations in the Nav1.7 gene underlie congenital indifference to pain in multiple human populations. *Clin. Genet. 71*, 311−319.
(35) Fischer, T.-Z., and Waxman, S.-G. (2010) Familial pain syndromes from mutations of the NaV1.7 sodium channel. *Ann. N. Y. Acad. Sci. 1184*, 196−207.
(36) Hille, B. (1972) The permeability of the sodium channel to metal cations in myelinated nerve. *J. Gen. Physiol. 59*, 637−58.
(37) Ulbricht, W. (2008) Effects of veratridine on sodium currents and fluxes. *Rev. Physiol. Biochem. Pharmacol. 133*, 1−54.
(38) Bregman, H., Berry, L., Buchanan, J.-L., Chen, A., Du, B., Feric, E., Hierl, M., Huang, L., Immke, D., Janosky, B., Johnson, D., Li, X., Ligutti, J., Liu, D., Malmberg, A., Matson, D., McDermott, J., Miu, P., Nguyen, H.-N., Patel, V.-F., Waldon, D., Wilenkin, B., Zheng, X.-M., Zou, A., McDonough, S.-I., and DiMauro, E.-F. (2011) Identification of a potent, state-dependent inhibitor of Nav1.7 with oral efficacy in the formalin model of persistent pain. *J. Med. Chem. 54*, 4427−4445.
(39) Chevrier, P., et al. (2004) Differential modulation of $Na_v1.7$ and $Na_v1.8$ peripheral nerve sodium channels by the local anesthetic lidocaine. *Br. J. Pharmacol. 142* (3), 576−584.
(40) Nau, C., et al. (1999) Stereoselectivity of bupivacaine in local anesthetic-sensitive ion channels of peripheral nerve. *Anesthesiology 91* (3), 786−795.
(41) Estacion, M., et al. (2010) Effects of ranolazine on wild-type and mutant hNav1.7 channels and on DRG neuron excitability. *Mol. Pain 6*, 35.
(42) McNulty, M. M., et al. (2004) State-dependent mibefradil block of Na+ channels. *Mol. Pharmacol. 66*, 1652−1661.
(43) Fischer, T. Z., et al. (2009) A novel Nav1.7 mutation producing carbamazepine-responsive erythromelalgia. *Ann. Neurol. 65* (6), 733−741.
(44) Sheets, P. L., et al. (2008) Differential block of sensory neuronal voltage-gated sodium channels by lacosamide [(2*R*)-2-(acetylamino)-*N*-benzyl-3-methoxypropanamide], lidocaine, and carbamazepine. *J. Pharmacol. Exp Ther. 326* (1), 89−99.
(45) Akiba, I1, Seki, T., Mori, M., Iizuka, M., Nishimura, S., Sasaki, S., Imoto, K., and Barsoumian, E. L. (2003) Stable expression and characterization of human PN1 and PN3 sodium channels. *Recept. Channels 9* (5), 291−299.
(46) Zhang, J.-H., Chung, T.-D., and Oldenburg, K.-R. (1999) A Simple Statistical Parameter for Use in Evaluation and Validation of High Throughput Screening Assays. *J. Biomol. Screening 4*, 67−73.
(47) Bhave, G., Lonergan, D., Chauder, B. A., and Denton, J. S. (2010) Small-molecule modulators of inward rectifier K+ channels: recent advances and future possibilities. *Future Med. Chem. 2* (5), 757−774.
(48) Ramos-Hunter, S. J., Engers, D. W., Kaufmann, K., Du, Y., Lindsley, C. W., Weaver, C. D., and Sulikowski, G. A. (2013) Discovery and SAR of a novel series of GIRK1/2 and GIRK1/4 activators. *Bioorg. Med. Chem. Lett. 23* (18), 5195−5198.
(49) Wen, W., Wu, W., Romaine, I. M., Kaufmann, K., Du, Y., Sulikowski, G. A., Weaver, C. D., and Lindsley, C. W. (2013) Discovery of "molecular switches" within a GIRK activator scaffold that afford selective GIRK inhibitors. *Bioorg. Med. Chem. Lett. 23* (16), 4562−4566.
(50) Wen, W., Wu, W., Weaver, C. D., and Lindsley, C. W. (2014) Discovery of potent and selective GIRK1/2 modulators via "molecular switches" within a series of 1-(3-cyclopropyl-1-phenyl-1H-pyrazol-5-yl)ureas. *Bioorg. Med. Chem. Lett. 24* (21), 5102−5106.

DOI: 10.1021/acschemneuro.5b00004
ACS Chem. Neurosci. 2015, 6, 871−878